Catalytically Important Ionizations along the Reaction Pathway of Yeast Pyrophosphatase†

Georgiy A. Belogurov,‡ Igor P. Fabrichniy,‡ Pekka Pohjanjoki,§ Vladimir N. Kasho,|| Erkka Lehtihuhta,§ Maria V. Turkina,‡ Barry S. Cooperman,⊥ Adrian Goldman,# Alexander A. Baykov,*,‡ and Reijo Lahti*,§

A. N. Belozersky Institute of Physico-Chemical Biology and School of Chemistry, Moscow State University, Moscow 119899, Russia, Department of Biochemistry, University of Turku, FIN-20014 Turku, Finland, Center for Ulcer Research and Education, Department of Medicine, University of California, Los Angeles, California 90073, Department of Chemistry, University of Pennsylvania, Pennsylvania 19104-6323, and Institute of Biotechnology, University of Helsinki, P.O. Box 56, FIN-00014 Helsinki, Finland

Received April 20, 2000; Revised Manuscript Received August 21, 2000

ABSTRACT: Five catalytic functions of yeast inorganic pyrophosphatase were measured over wide pH ranges: steady-state PP_i hydrolysis (pH 4.8−10) and synthesis (6.3−9.3), phosphate−water oxygen exchange (pH 4.8−9.3), equilibrium formation of enzyme-bound PP_i (pH 4.8−9.3), and Mg^{2+} binding (pH 5.5−9.3). These data confirmed that enzyme−PP_i intermediate undergoes isomerization in the reaction cycle and allowed estimation of the microscopic rate constant for chemical bond breakage and the macroscopic rate constant for PP_i release. The isomerization was found to decrease the pK_a of the essential group in the enzyme−PP_i intermediate, presumably nucleophilic water, from >7 to 5.85. Protonation of the isomerized enzyme−PP_i intermediate decelerates PP_i hydrolysis but accelerates PP_i release by affecting the back isomerization. The binding of two Mg^{2+} ions to free enzyme requires about five basic groups with a mean pK_a of 6.3. An acidic group with a pK_a ∼ 9 is modulatory in PP_i hydrolysis and metal ion binding, suggesting that this group maintains overall enzyme structure rather than being directly involved in catalysis.

Yeast (*Saccharomyces cerevisiae*) pyrophosphatase (EC 3.6.1.1; Y-PPase)[1] belongs to a group of enzymes that catalyze reversible phosphoryl transfer from polyphosphates to water and are basic to cell energetics. Y-PPase is a homodimer containing 286 amino acid residues per monomer (*1*). The active site of Y-PPase contains 14 polar residues that structurally align very well with the corresponding conserved residues in PPases from *Escherichia coli* (E-PPase) (*2*), *Thermus thermophilus* (*3*), and *Sulfolobus acidocaldarius* (*4*). Y-PPase requires divalent metal ions for catalysis, with Mg^{2+} conferring the highest activity (*5*) and is active with either three or four magnesium ions per active site (*6*−*8*). Two divalent metal ions (M1 and M2) per active site have been identified in the "resting" enzyme by X-ray crystallography and four metal ions (M1-M4) and two phosphates (P1 and P2) in the product complex of Y-PPase (*2*, *9*).

The sequence of catalytic events in the active site includes substrate ($MgPP_i$ or Mg_2PP_i) binding to preformed enzyme complex containing Mg^{2+} at sites M1 and M2, isomerization of the resulting complex, P−O bond breakdown by direct attack of water and stepwise dissociation of two phosphate molecules (Scheme 1) (*10*). The rate constants in Scheme 1 can be estimated from steady state and equilibrium measurements (*10*−*12*).

PPase activity exhibits a bell-shaped dependence on pH. The identity of the ionizable groups responsible for this dependence and the catalytic steps at which they participate are unknown. A proposed candidate for the essential basic group is a Mg^{2+}-coordinated hydroxide ion, a possible nucleophile attacking PP_i at the k_3 step (*13*, *14*). This proposal is supported by structural studies of Y-PPase showing a water molecule or a hydroxide ion to be coordinated to the metal ions M1 and M2 and Asp117 and placed in a suitable position for an attack on PP_i (*2*) and by inhibition studies indicating that fluoride ion, which could compete with OH^- for binding to Mg^{2+}, strongly inhibits PPases (*10*, *15*). On the other hand, in *E. coli* PPase, whose functional properties are very similar to those of Y-PPase, k_3 remains constant over the pH range 6.5−9.3 at high Mg^{2+} concentration (20 mM) (*16*, *17*). This may mean that the pK_a of the nucleophilic water hydroxide ion is below 6.5 or greater than 9.3 or that the essential basic group participates at some other step.

Y-PPase is better suited for the analysis of the pH dependence of catalysis than E-PPase. First, E-PPase undergoes dissociation into trimers at pH <6.5 (*18*), with severe

† This work was supported by grants from the Russian Foundation for Basic Research (97-04-48487, 00-04-48310, and 00-15-97907), the Finnish Academy of Sciences (35736 and 47513) and NIH (TW00407).

* To whom correspondence should be addressed. (A.A.B.) Phone: 095-939-5541. Fax: 095-939-3181. E-mail: baykov@genebee.msu.su. (R.L.) Phone: 358-2-333-6845. Fax: 358-2-333-6860. E-mail reijo.lahti@utu.fi.

‡ Moscow State University.

§ University of Turku.

|| University of California.

⊥ University of Pennsylvania.

University of Helsinki.

[1] Abbreviations: E-PPase, *Escherichia coli* inorganic pyrophosphatase; PPase, inorganic pyrophosphatase; P_i, inorganic phosphate; PP_i, inorganic pyrophosphate; Y-PPase, yeast (*Saccharomyces cerevisiae*) inorganic pyrophosphatase.

10.1021/bi000895s CCC: $19.00
Published on Web 10/14/2000

Scheme 1: PP_i-P_i Equilibration by PPase[a]

$$(EM_2)_t \underset{k_2}{\overset{k_1}{\rightleftharpoons}} (EM_{n+2}PP^*)_t \underset{k_B}{\overset{k_A}{\rightleftharpoons}} (EM_{n+2}PP)_t \underset{k_4}{\overset{k_3}{\rightleftharpoons}} (EM_{n+2}P_2)_t \underset{k_6}{\overset{k_5}{\rightleftharpoons}} (EM_{n+1}P)_t \underset{k_8}{\overset{k_7}{\rightleftharpoons}} (EM_2)_t$$

[a] E = enzyme, M = Mg^{2+}, PP = PP_i, P = P_i, n = 1 or 2. Subscript t refers to all protonated forms of the indicated species.

consequences for activity (*19*), which precludes kinetic analysis at acidic pH values, whereas Y-PPase preserves its structure down to pH 4.8. Second, the pH-optimum of activity for Y-PPase (6.5−7) is lower than for E-PPase (8.5−9), allowing a more comprehensive analysis in the alkaline region. The results reported below suggest that hydrolysis of the enzyme-bound PP_i becomes the rate-limiting step in the acidic pH region and also show that the ionizable group modulating activity in the alkaline region is not essential for catalysis.

EXPERIMENTAL PROCEDURES

Enzyme. Y-PPase was purified from the overproducing *E. coli* XL2blue[b] strain transformed with a vector including the coding region of yeast *IPP1* gene under the *tac* promoter as described by Heikinheimo et al. (*20*). Enzyme concentration was calculated on the basis of the subunit molecular mass of 32 kDa (*1*) and $A_{280}^{1\%}$ equal to 14.5 (*5*) or by the Bradford (*21*) assay.

Methods. PP_i hydrolysis was assayed by continuously recording P_i liberation with an automatic P_i analyzer (*22*). Enzyme concentration was varied in order to get comparable absorbance values at different substrate and metal ion concentrations.

PP_i synthesis was assayed continuously by a coupled-enzyme procedure (*23*), using ATP-sulfurylase to convert PP_i formed into ATP and luciferase to monitor ATP formation. The assay mixture of 0.2 mL volume contained 20 mM potassium phosphate, 5 mM free Mg^{2+}, 5 μL of luciferin/luciferase solution (Sigma ATP assay mix, catalog no. FL-ASC, reconstituted with 5 mL of water), 0.7 units/mL ATP-sulfurylase (Sigma), 10 μM adenosine-5′-phosphosulfate, 1 mM dithiothreitol, 1 mg/mL bovine serum albumin, and buffer. The reaction was initiated by adding PPase, and the time course of luminescence was followed with an LKB model 1250 luminometer. However, luciferase instability at pH 6.3 and 9.3 necessitated use of a two-step procedure. First, PP_i synthesis was carried out and the synthesized PP_i was converted into ATP in the assay mixture described above but lacking the luciferin/luciferase reagent, and second, the ATP formed was assayed at pH 8.0. To this end, 30 μL aliquots of the incubation mixture were withdrawn at 5-min intervals over 30 min, quenched with 30 μL of 1 M trifluoroacetic acid, incubated for 3−5 min at room temperature, and neutralized with 30 μL of 1.5 M Tris. A 20-μL aliquot of the resulting mixture was added to 0.2 mL of 0.2 M Tris-HCl buffer (pH 8.0) containing 5 μL of the luciferin/luciferase solution and 30 μM EGTA, and the luminescence was measured. Care was taken that ATP-sulfurylase concentration was sufficiently high, so that PP_i conversion into ATP proceeded at least 20 times faster than PP_i formation.

Mg^{2+} binding was assayed by equilibrium microdialysis in combination with atomic absorption spectroscopy to measure Mg content in the dialysis chambers (*16*). The ratio of the volumes of the chambers with and without enzyme was 1:130, allowing precise control of free metal ion concentration at its micromolar levels. Procedures used to measure enzyme-bound PP_i formation at equilibrium (*12*) and enzyme-catalyzed oxygen exchange (*17*) were as described previously.

Table 1: pH-Dependent Values of Dissociation Constants for Mg^{2+} Complexes of PP_i and P_i in the Presence of 50 mM K^+[a]

pH	K_{A1}[b] (mM)	K_{A2}[b] (mM)	K_B[c] (mM)
4.8	4.47	463	148
5.5	1.74	53.8	80
6.3	0.477	8.87	26
7.2	0.1123	2.84	8.5
8.5	0.0102	2.04	6.1
9.3	0.004 44	2.01	6.0
10.0	0.003 56	2.00	6.0

[a] Definitions (the subscript t refers to total concentration, i.e., all species having the stoichiometry shown without regard to protonation state): $K_{A1} = [Mg][PP_i]_f/[MgPP_i]_t$; $K_{A2} = [Mg][MgPP_i]_f/[Mg_2PP_i]$; $K_B = [Mg][P_i]_f/[MgP_i]_t$. [b] Baykov et al. (*24*). [c] Calculated on the basis of the value at pH 7.2 (*25*−*26*), assuming that $MgHPO_4$ is the only form of magnesium phosphate present at pH >5.5; at pH ≤5.5 formation of $MgH_2PO_4^+$ with a dissociation constant of 190 mM was taken into account (*27*).

The following pH buffers were used in metal binding and PP_i hydrolysis studies (0.1 M ionic strength, 50 mM K^+), except as noted: 95 mM acetic acid/KOH, 100 μM EGTA (pH 4.8); 63 mM MES/KOH, 37 mM KCl, 100 μM EGTA (pH 5.5); 40 mM PIPES/KOH, 100 μM EGTA (pH 6.3); 83 mM TES/KOH, 17 mM KCl, 50 μM EGTA (pH 7.2); 90 mM TAPS/KOH, 5 μM EGTA (pH 8.5); 52 mM TAPS/KOH, 48 mM CAPS/KOH (pH 9.3); 70 mM CAPS/KOH, 30 mM KCl (pH 10.0). The rationale for keeping K^+ concentration at a constant level was that K^+ forms a relatively tight complex with PP_i (*24*), which might bind to enzyme. The media used in incubations with P_i (oxygen exchange and synthesis of free and enzyme-bound PP_i) were prepared by mixing appropriate volumes of 100 mM potassium phosphate, 100 mM $MgCl_2$, and the buffers mentioned above, except that 20 mM acetic acid/KOH buffer was used at pH 4.8 and appropriate volumes of 1 M KOH were added to neutralize protons released upon Mg^{2+}-acetate complex formation.

Calculations and Data Analysis. Values of the apparent equilibrium constants used to calculate the concentrations of free Mg^{2+}, $MgPP_i$, and Mg_2PP_i in the presence of 50 mM K^+ at different pH values are presented in Table 1. At pH 4.8, Mg^{2+} binding by acetate was taken into consideration, using the apparent dissociation constant of 155 mM, which was calculated from the pH shift caused by addition of $MgCl_2$ to the acetate buffer. Fitting of various equations to data was performed using the program SCIENTIST (MicroMath) or the program described by Duggleby (*28*).

The dependence on [Mg^{2+}] and pH of Mg^{2+} binding to free enzyme and of the measured values of the catalytic constant (k_h) for PP_i hydrolysis is well described by Scheme

Scheme 2: pH and Mg^{2+} Dependence of PPase Catalysis of PP_i Hydrolysis

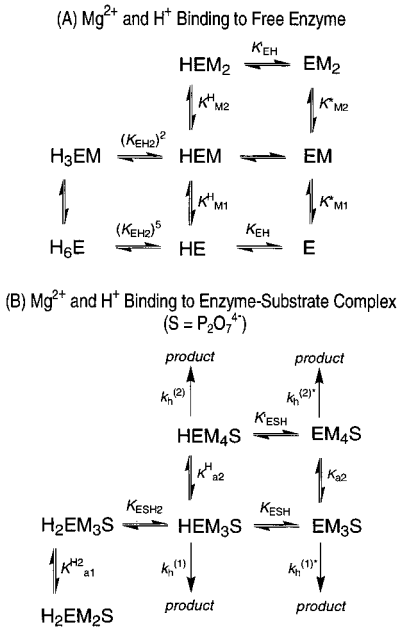

2. In this scheme, enzyme species lacking substrate are assumed to be in equilibrium with one another, as are all enzyme−substrate species. The very sharp decrease in Mg^{2+} binding as pH decreases below 7 is attributed to the involvement of the conjugate bases of five acidic groups, which for simplicity are assumed to have the same ionization constant K_{EH2}. Three of these groups must deprotonate in order to bind the first Mg^{2+} and the other two must deprotonate to bind the second Mg^{2+}. Other assumptions of the model and details of the fitting procedure were as described previously for *E. coli* PPase (*17*, *29*).

Values of the dissociation constants for Mg^{2+} binding to two sites on Y-PPase at fixed pH were estimated by fitting equilibrium dialysis data to eq 1, where n measures the number of Mg^{2+} ions bound per monomer and the parameters K_{M1} and K_{M2} are apparent dissociation constants at fixed pH. Equation 1 is a rearranged form of the Adair equation for two sites.

$$n = \frac{1 + 2[Mg^{2+}]/K_{M2}}{1 + K_{M1}/[Mg^{2+}] + [Mg^{2+}]/K_{M2}} \quad (1)$$

Fitting n as a function of both pH and $[Mg^{2+}]$, according to Scheme 2A, was accomplished by making the following substitutions:

$$K_{M1} = K_{M1}^{H}\frac{1 + ([H^+]/K_{EH2})^5 + K_{EH}/[H^+]}{1 + ([H^+]/K_{EH2})^2} \quad (2)$$

$$K_{M2} = K_{M2}^{H}\frac{1 + ([H^+]/K_{EH2})^2}{1 + K'_{EH}/[H^+]} \quad (3)$$

Values of k_h as a function of both pH and $[Mg^{2+}]$ were fit to eq 4, derived from Scheme 2B, where $a = 1 + K_{ESH}/[H^+] + (1 + K'_{ESH}/[H^+])[Mg^{2+}]/K_{a2}^{H} + (1 + K_{a1}^{H2}/[Mg^{2+}])[H^+]/K_{ESH2}$.

$$k_h = \{k_h^{(1)} + k_h^{(1)*}K_{ESH}/[H^+] + (k_h^{(2)} + k_h^{(2)*}K'_{ESH}/[H^+])[Mg^{2+}]/K_{a2}^{H}\}/a \quad (4)$$

Values of k_3 were evaluated from eq 5 (*10*), where v_{ex} is the rate of P_i-H_2O oxygen exchange at an arbitrary P_i concentration, f_{epp} is the equilibrium amount of enzyme-bound PP_i formed at equilibrium with solution P_i (taken at the same concentration), $K_{AB} = k_A/k_B$ (see Scheme 1). The partition coefficient $P_c = k_4/(k_5 + k_4)$ is estimated from oxygen exchange data (*30*). At pH ≥7.2, $K_{AB} > 25$ (*10*) and the term $1 + 1/K_{AB}$ in the numerator could be neglected. At lower pH values, the species designated as $EM_{n+2}PP^*$ in Scheme 1 becomes protonated (*10*). As a result, K_{AB} decreases substantially and $1/K_{AB}$ becomes comparable with unity. In these conditions, the value of K_{AB} could be approximated by $K_{ES}/[H^+]$, where K_{ES}, the apparent acid dissociation constant for the PP_i-containing enzyme (the sum of $EM_{n+2}PP^*$ and $EM_{n+2}PP$ in Scheme 1), is equal to $10^{-5.4 \pm 0.2}$ M (*10*). This approximation makes use of the observation that at pH ≤6.3 the concentrations of $EM_{n+2}PP$ and of protonated $EM_{n+2}PP^*$ exceed by far the concentration of deprotonated $EM_{n+2}PP^*$ (*10*).

$$k_3 = \frac{v_{ex}(1 - 0.75P_c)(1 + 1/K_{AB})}{f_{epp}(1 - P_c)[E]_0} \quad (5)$$

Fitting of k_3 and $k_{pp,off} = v_s/f_{epp}[E]_t$ as functions of pH was accomplished with eq 6, where p is the apparent value of k_3 or $k_{pp,off}$; p^{OH}, p^{H}, and p^{H2} are their values for deprotonated, monoprotonated, and diprotonated enzyme, respectively; K_{H1} and K_{H2} are the corresponding acid dissociation constants.

$$p = \frac{p^{H} + p^{OH}K_{H1}/[H^+] + p^{H2}[H^+]/K_{H2}}{1 + K_{H1}/[H^+] + [H^+]/K_{H2}} \quad (6)$$

RESULTS

Mg^{2+} Binding. Equilibrium dialysis measurements carried out at 0.5−2000 μM free Mg^{2+} concentrations have indicated the presence of two metal-binding sites per subunit over the pH range 5.5−9.3 (Figure 1). Binding to both sites, as characterized by the apparent dissociation constants K_{M1} and K_{M2}, was pH dependent (Table 2). Binding of M1 exhibited a pH optimum, whereas binding of M2 appeared to progressively increase with pH (Table 2).

These preliminary conclusions were confirmed by computer modeling, which yielded a minimal binding scheme describing the whole set of data in Figure 1 (Scheme 2A) and permitted evaluation of the equilibrium constants K_{EH2}, K_{M1}^{H}, K_{M2}^{H}, K_{EH}, and $K'_{EH,}$ as well as of a lower limit for K_{M1}^{*} and an upper limit for K_{M2}^{*} (Table 3). The sharp increase in both K_{M1} and K_{M2} in acidic medium (Table 2) is attributed to the involvement of the conjugate bases of five acidic groups, which for simplicity are assumed to have the same ionization constant K_{EH2} (see *Calculations and Data Analysis*). Fits to the data were poorer if fewer than five groups were involved, and were not improved by allowing deprotonation of H_6E and H_3EM to proceed with different dissociation constants. These five groups are presumably active site Asp and Glu ligands of Mg^{2+} which have been identified by X-ray crystallography (*2*, *9*). At neutral pH,

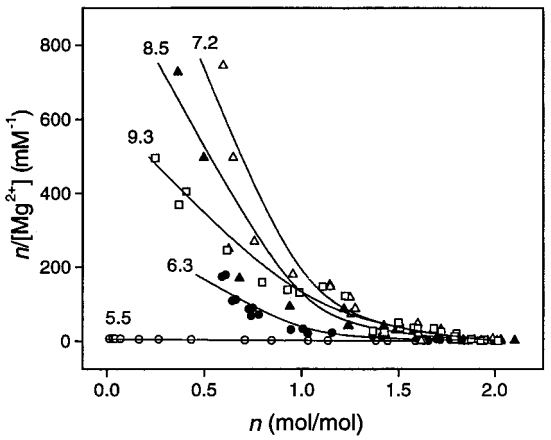

FIGURE 1: Scatchard plots of Mg^{2+} binding to Y-PPase at fixed pH values. Lines are drawn to eq 1, using parameter values found in Table 3. Experimental conditions: [PPase], 50−500 μM; [Mg^{2+}], 0.5−2000 μM. Values of pH are shown on the curves.

Table 2: Metal Ion Binding Constants Estimated by Equilibrium Dialysis

pH	K_{M1} (μM)	K_{M2} (μM)
5.5	210 ± 30	1600 ± 200
6.3	3.2 ± 0.2	210 ± 30
7.2	0.7 ± 0.1	34 ± 6
8.5	1.1 ± 0.2	49 ± 12
9.3	2.3 ± 0.5	15 ± 5
7.2[a]	1.0 ± 0.1	53 ± 8

[a] Measured in 0.1 M Tris/HCl buffer.

Table 3: Equilibrium and Rate Constants for Scheme 2

	value	
parameter	yeast PPase	*E. coli* PPase[a]
K^*_{M1} (μM)	>10	
K^*_{M2} (μM)	<4	24 ± 3
K^H_{M1} (μM)	0.9 ± 0.1	12 ± 2
K^H_{M2} (μM)	26 ± 3	9000 ± 1000
pK_{EH}	9.0 ± 0.2	> 10
pK'_{EH}	9.2 ± 0.2	7.4 ± 0.5
pK_{EH2}	6.27 ± 0.02	7.11 ± 0.05
K_{a2} (mM)	2.8 ± 1.0	4.1 ± 0.7
K^H_{a2} (mM)	0.8 ± 0.3	>50
K^{H2}_{a1} (mM)	0.35 ± 0.06	0.6 ± 0.1
pK_{ESH}	7.6 ± 0.1	
pK'_{ESH}	8.2 ± 0.2	9.90 ± 0.05
pK_{ESH2}	6.4 ± 0.1	7.17 ± 0.04
$k^{(1)}_h$ (s^{-1})	770 ± 130	≤100
$k^{(2)}_h$ (s^{-1})	220 ± 10	320 ± 20
$k^{(1)*}_h$ (s^{-1})	84 ± 3	
$k^{(2)*}_h$ (s^{-1})	31 ± 5	

[a] Baykov et al. (*29*).

the monoprotonated enzyme species HE, HEM and HEM_2 predominate.

k_h Dependence on [Mg^{2+}] and pH. At fixed free Mg^{2+} concentration (0.01−40 mM), the dependence of the hydrolysis rate on the sum of [$MgPP_i$]and [Mg_2PP_i] obeyed the Michaelis−Menten equation, yielding the k_h and $k_h/K_{m,h}$ values shown in Figure 2. Computer analysis of k_h dependence on [Mg^{2+}] and pH leads to Scheme 2B, having four catalytically active species, the catalytic efficiencies of which decrease in the order HEM_3S > HEM_4S > EM_3S > EM_4S (Table 3). The bell-shaped curves near neutrality (pHs 6.3 and 7.2) largely reflect conversion of the catalytically inactive complex H_2EM_2S first to the most active complex HEM_3S and ultimately to the less active complex HEM_4S. Similar pH-profiles for k_h measured at 20 mM Mg^{2+} were previously reported for several active site variants of Y-PPase (*14*). At lower pH (4.8 and 5.5) only an increase with increasing [Mg^{2+}] is seen (HEM_3S formation), since even 40 mM Mg^{2+} is insufficient to permit binding of a fourth Mg^{2+} to the enzyme·substrate complex. Finally, at basic pH (8.5−10.0), even 10 μM Mg^{2+} is sufficient to bind three Mg^{2+} to the enzyme−substrate complex, and the decrease in k_h reflects conversion of a mixture of the more active HEM_3S and EM_3S complexes to the less active HEM_4S and EM_4S complexes, respectively.

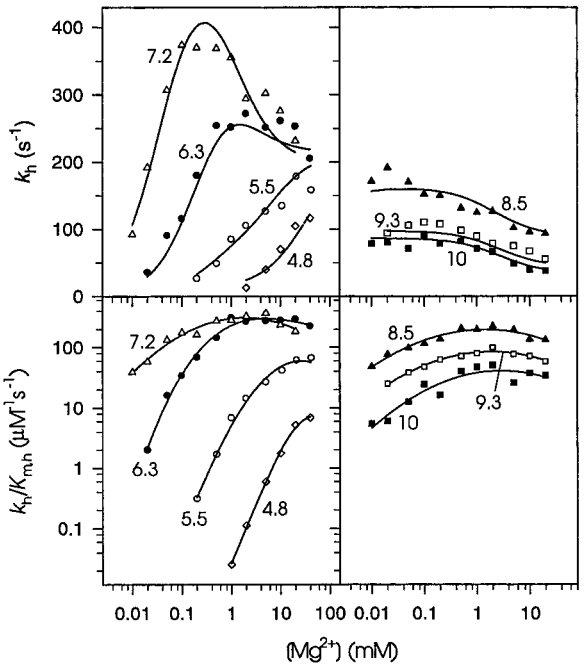

FIGURE 2: Dependencies of k_h and $k_h/K_{m,h}$ for Y-PPase on [Mg^{2+}] at fixed pH values. Values of $k_h/K_{m,h}$ are expressed in terms of the sum of $MgPP_i$ and Mg_2PP_i concentrations. The lines for k_h are drawn to eq 4, using parameter values found in Table 3. Values of pH are shown on the curves.

k_3 and $k_{pp,off}$ Dependence on [Mg^{2+}] and pH. Equation 5 allowed evaluation of k_3, the rate constant for chemical bond breakage in Scheme 1, from three combined sets of data: rates of P_i-H_2O oxygen exchange (v_{ex}), distribution of the P_i forms having different number (from zero to four) of exchanged O atoms during the exchange (as characterized by P_c), and the equilibrium amount of enzyme-bound PP_i formed at equilibrium with solution P_i (f_{epp}) (Table 4). Also evaluated was $k_{pp,off} = v_s/f_{epp}[E]_t$, the overall rate constant for PP_i release from its two complexes with Y-PPase (see Discussion). These evaluations were subject to two limitations. First, f_{epp} could not be accurately estimated at low Mg^{2+} concentrations (<2 mM) and at pH 10. Second, the ATP-sulfurylase used in v_s measurements was inactivated outside the pH range 6.3−9.3.

Values of k_3 and $k_{pp,off}$ show only small variations with [Mg^{2+}] but are clearly pH dependent (Table 4). The pH profiles for k_3 and $k_{pp,off}$ are shown in Figure 3A, in which the lines are derived by fitting to eq 6. The pH profile for k_h is shown for comparison. At pH 4.8, the profiles for k_3 and k_h approach each other, consistent with the k_3 step becoming

Table 4: Estimation of k_3 and $k_{pp,off}$ for Y-PPase

pH	$[Mg^{2+}]$ (mM)[a]	$[P_i]$ (mM)[b]	k_h (s^{-1})	$v_{ex}/[E]_t$ (s^{-1})	P_c	f_{epp} (%)	$v_s/[E]_t$ (s^{-1})	k_3 (s^{-1})[c]	$k_{pp,off}$ (s^{-1})
4.8	40	20	117 ± 2	0.113 ± 0.007	0.043 ± 0.002	0.4 ± 0.1		140 ± 50	
5.5	40	10	158 ± 5	4.8 ± 0.1	0.052 ± 0.007	1.90 ± 0.2		450 ± 60	
5.5	20	10	178 ± 4	2.07 ± 0.02	0.046 ± 0.003	1.1 ± 0.1		350 ± 40	
5.5	10	10	135 ± 3	1.02 ± 0.03	0.048 ± 0.003	0.55 ± 0.14		330 ± 90	
6.3	40	10	205 ± 7	74 ± 1	0.124 ± 0.008	8.8 ± 0.6	21 ± 1	980 ± 90	240 ± 30
6.3	20	10	253 ± 14	71 ± 1	0.121 ± 0.002	6.7 ± 0.9	14 ± 3	1200 ± 200	210 ± 70
6.3	10	10	262 ± 10	48 ± 1	0.093 ± 0.003	3.9 ± 0.4	5.6 ± 2.0	1400 ± 200	140 ± 40
6.3	5	10	251 ± 12	30 ± 1	0.074 ± 0.002	2.0 ± 0.1	2.8 ± 0.3	1720 ± 130	140 ± 20
7.2	20	2	231 ± 6	56 ± 3	0.35 ± 0.04	4.7 ± 0.5	1.39 ± 0.01	1360 ± 300	30 ± 3
7.2	10	2	276 ± 5	44 ± 1	0.342 ± 0.003	3.9 ± 0.2	1.23 ± 0.05	1270 ± 80	31 ± 2
7.2	5	2	302 ± 9	27 ± 1	0.293 ± 0.007	2.76 ± 0.02	0.94 ± 0.04	1060 ± 40	34 ± 2
7.2	2	2	294 ± 10	10.9 ± 0.4	0.265 ± 0.006	1.18 ± 0.05	0.39 ± 0.05	1000 ± 90	33 ± 6
8.5	20	2	93 ± 3	31 ± 1	0.314 ± 0.004	5.9 ± 0.5	0.38 ± 0.02	590 ± 60	6.5 ± 0.9
8.5	10	2	96 ± 4	35 ± 1	0.33 ± 0.02	7.0 ± 0.2	0.37 ± 0.01	570 ± 60	5.2 ± 0.3
8.5	5	2	102 ± 2	33 ± 1	0.337 ± 0.004	6.1 ± 1.0	0.39 ± 0.02	610 ± 120	6.3 ± 1.3
8.5	2	2	127 ± 4	22.4 ± 0.16	0.333 ± 0.003	4.3 ± 0.8	0.312 ± 0.002	580 ± 110	7.2 ± 1.3
9.3	20	1	56 ± 2	5.6 ± 0.2	0.204± 0.001	2.2 ± 0.5	0.073 ± 0.002	270 ± 60	3.3 ± 0.7
9.3	10	1	68 ± 4	8.3 ± 0.3	0.26 ± 0.02	3.0 ± 0.5	0.061 ± 0.003	300 ± 70	2.0 ± 0.4
9.3	5	1	75 ± 2	8.0 ± 0.1	0.234 ± 0.003	2.6 ± 0.1	0.059 ± 0.003	340 ± 20	2.3 ± 0.2
9.3	2	1	79 ± 1	7.0 ± 0.2	0.269 ± 0.004	1.86 ± 0.15	0.049 ± 0.002	410 ± 50	2.6 ± 0.3
7.2[d]	20	2	250 ± 15	30 ± 3	0.317 ± 0.009	2.1 ± 0.5	0.67 ± 0.05	1600 ± 600	32 ± 10

[a] Concentration of free ion. [b] Total concentration of P_i used in measurements of v_{ex}, P_c, v_s, and f_{epp}. [c] Estimated with eq 5. [d] Measured in 0.1 M Tris/HCl buffer.

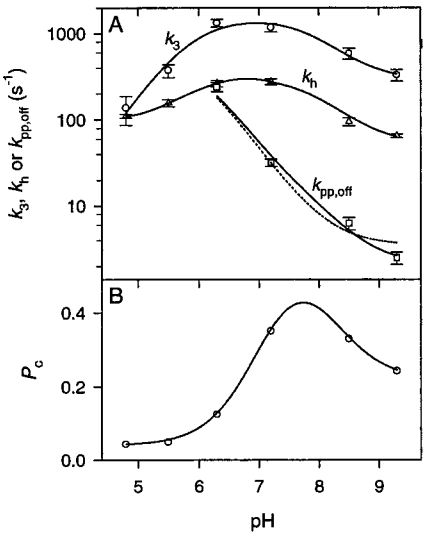

FIGURE 3: Dependencies of k_h, $k_{pp,off}$, k_3, and P_c on pH**.** Parameter values are from Table 4 and averaged over the Mg^{2+} concentration range used. The lines for $k_{pp,off}$, k_3, and P_c are drawn to eq 6, using parameter values found in Table 5 (see text for details).

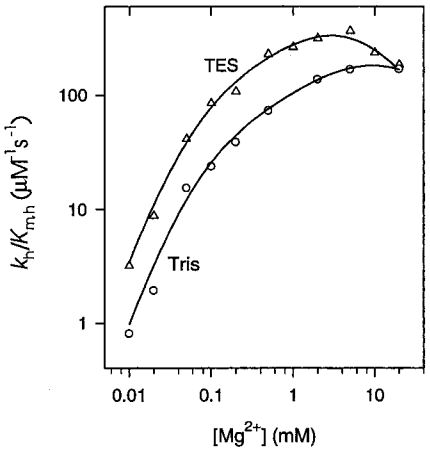

FIGURE 4: Buffer effect on the Mg^{2+} concentration dependencies of $k_h/K_{m,h}$ for Y-PPase at pH 7.2. Open circles, 0.1 M Tris/HCl; open triangles, 0.1 M TES/KOH.

exclusively rate limiting in PP_i hydrolysis. The pH profile for k_3 indicates a requirement for a basic and an acidic groups with pK_as of 5.85 and 7.9, respectively. The pH-profile for $k_{pp,off}$ could be well described by assuming two acidic groups with the same pK_a values (5.85 and 7.9) and three nonzero rate constants corresponding to the three protonation states of the enzyme·PP_i species (solid line in Figure 3A). Assuming only one acidic group resulted in a poorer fit in the alkaline medium (dotted line in Figure 3A).

Buffer Effect on Y-PPase. Most previous work on Y-PPase was done in Tris and similar amino alcoholic buffers, which, by contrast with the zwitterionic buffers used in the present work, markedly affect metal ion and substrate binding to *E. coli* PPase (*29*). The data presented in Table 2 and Figure 4 show only modest Tris effects on Mg^{2+} binding constants and $k_h/K_{m,h}$ for Y-PPase at pH 7.2, which contrast with the larger effects seen on *E. coli* PPase (*29*). Neither k_h nor k_3 were affected (Table 4). The $[Mg^{2+}]$ dependence of $k_h/K_{m,h}$ for recombinant Y-PPase in the presence of Tris (Figure 4) was quite similar to that reported previously for Y-PPase isolated from normal yeast (*8*). The $[Mg^{2+}]$ dependencies of k_h were also very similar.

DISCUSSION

The minimal scheme of pyrophosphatase catalysis of PP_i hydrolysis (Scheme 1) involves Mg^{2+} binding to multiple sites on enzyme, substrate binding, isomerization of the resulting complex, substrate hydrolysis, and P_i release. In the present work, we measured the pH dependence of some of these steps to estimate the pK_a values for the protein groups involved. Below we correlate this information with the three-dimensional structure of the enzyme reported previously (*2*).

Mg^{2+} Binding. As determined by X-ray crystallography, the two activating metal ions which bind to the active site

of Y-PPase in the absence of substrate occupy the sites M1 and M2. At the M1 site, both Mn^{2+} and Mg^{2+} are coordinated to three Asp residues (115, 120, and 152) and via water to Asp117 (*2*, *9*, *31*). For the M2 site, data are only available for Mn^{2+} ion, which is directly coordinated only to Asp120 and via water to Glu48 and Asp117 (*2*). The binding data reported above indicate the requirement for three ionizable groups in M1 binding and two more in M2 binding and are thus in a good agreement with the structure. The mean pK_a value of these groups derived from the binding data (6.27) is quite high for a carboxylate, but again is in accordance with the structure: the negative charge density is quite high in the active site and most of the carboxylates can participate in hydrogen bonding in the apoenzyme (*2*, *9*, *31*). The five unprotonated groups required for Mg^{2+} binding may be thus metal ligands. By contrast, the group with a pK_a of 9.0−9.2 facilitates binding when in the protonated form, ruling out its being a metal ligand. This group is likely to control the overall protein structure, consistent with the observation that deprotonation of this group induces positive cooperativity in M1 and M2 binding ($K^*_{M1} > K^*_{M2}$, whereas $K^H_{M1} < K^H_{M2}$; Table 3). The same group, having a p$K_{ESH} = 7.6$, appears to control Mg^{2+} binding in the enzyme−substrate complex, as suggested by the observation that its protonation also increases Mg^{2+} binding affinity ($K_{a2} > K^H_{a2}$). The identity of this group in the Y-PPase structure remains to be determined.

The high affinity of the M1 site for Mg^{2+} explains the reported difficulty in removing magnesium from Y-PPase by dialysis in the absence of EDTA (*32*), as well as the observation that Y-PPase crystals grown in the absence of added metal salt contain Mg^{2+} at site M1 (*31*). Y-PPase may be thus considered to be a Mg-metalloenzyme. Partial occupancy of the M1 site in the enzyme preparations used in fluorescence titrations of Y-PPase (*33*−*34*) may explain why this method gave a nearly 30-fold greater K_{M1} value at pH 7.2−7.4 compared to the value obtained in the present study. This explanation is supported by the observation that EDTA had a large opposite effect on Y-PPase fluorescence by comparison with Mg^{2+} (*32*).

There are two major differences in the Mg^{2+}-binding properties of Y-PPase and E-PPase. First, Y-PPase binds only two Mg^{2+} ions in the active site while E-PPase binds, in addition, one Mg^{2+} ion per pair of subunits in the subunit interface (*19*). Second, Y-PPase binds metal ions to the M1 and M2 sites 37- and 190-fold more tightly, respectively, than E-PPase at pH 7.2 (*29*). The difference between Y- and E-PPase in the affinity to M1 may be explained by the M1−Asp120/70 distance in monomagnesium enzyme being much shorter (2.11 Å) in Y-PPase (*31*) than in E-PPase [3.22 Å (*35*)]. In E-PPase part of the binding energy may be used to decrease the M1−Asp70 distance to 2.19 Å, as determined in the $EMg_{2.5}$ structure (*36*). M2 binding in E-PPase may also involve a conformational change, as suggested by a large change in Tyr absorbance upon the binding (*37*). As a consequence of low affinity of the M2 site in E-PPase, Mg_2-PP_i is more important as substrate for this enzyme.

$k_h/K_{m,h}$ and Substrate Binding. In earlier kinetic analyses of PPase, based on a scheme that did not include the species $EM_{n+2}PP^*$ (*17*, *29*), k_1, the rate constant for substrate binding, could be equated to $k_h/K_{m,h}$. However, for Scheme 1 the expression for $k_h/K_{m,h}$ is more complex (eq 7), so that

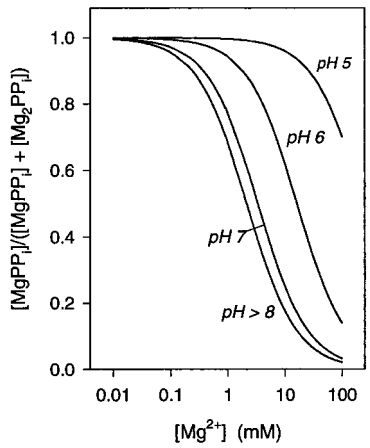

FIGURE 5: Distribution of PP_i between mono- and dimagnesium complexes as a function of pH and Mg^{2+} concentration. The lines were calculated from the binding constants listed in Baykov et al. (*24*).

Scheme 3: Ionizations of Reaction Intermediates in PPase Catalysis

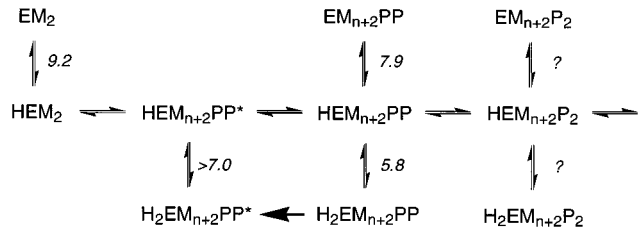

Table 5: pH Profile Parameters Estimated with Eq 6[a]

	p^{H2}	p^H	p^{OH}	pK_{H2}	pK_{H1}
k_3	0	1500 ± 300	290 ± 20	5.8 ± 0.3	7.9 ± 0.3
$k_{pp,off}$	630 ± 250	16 ± 11	2.1 ± 1.1	5.8[b]	7.9[b]
P_c	0.04 ± 0.01	0.57 ± 0.04	0.22 ± 0.01	7.0 ± 0.1	8.2 ± 0.1

[a] Units for k_3 and $k_{pp,off}$ are s^{-1}. [b] Constrained at this value.

rationalization of the complex pH and $[Mg^{2+}]$ dependence of this parameter (Figure 2) in terms of discrete effects on individual rate constants is beyond the scope of our present results.

$$\frac{k_h}{K_{m,h}} = \frac{k_1 k_A}{k_2[1 + k_B/k_3(1 - P_c)]} \quad (7)$$

In the enzyme−substrate complex, PP_i is coordinated to all four metal ions shown in Scheme 2B (*2*, *9*), consistent with both monomagnesium and dimagnesium complexes of PP_i, formed in comparable amounts under physiological conditions (Figure 5), being substrates for PPase. It should be noted that none of the substrate species is bound intact: a metal ion is coordinated to three oxygens of PP_i in the crystal structure of Mg_2PP_i (*38*) and to only two oxygens in the enzyme−substrate complex (*2*, *9*).

Substrate Conversion. Scheme 3 summarizes all the ionizations seen in the reaction intermediates and the respective pK_a values. The pK_a value shown for EM_2 was obtained from the analysis of Mg^{2+} binding (pK'_{EH} in Table 3), the pK_a values shown for $EM_{n+2}PP$ were deduced from the pH-dependence of k_3 (Figure 3A and Table 5), and the pK_a value shown for $EM_{n+2}PP^*$ was obtained from studies of fluoride binding to Y-PPase during catalysis (*10*). A

completely deprotonated $EM_{n+2}PP^*$ species, may also exist, but we have no evidence for that. The ionizations shown for $HEM_{n+2}P_2$ are evident from the bell-shaped pH dependence of P_c (Figure 3B), which is a function of k_4 and k_5, both referring to $HEM_{n+2}P_2$. However, as P_c depends on both k_4 and k_5, the pK_a values derived with eq 6 from the dependence of P_c on $[H^+]$ and shown in Table 5 include the rate constants k_4 and k_5 for $EM_{n+2}P_2$, $HEM_{n+2}P_2$, and $H_2EM_{n+2}P_2$ and are thus apparent, as demonstrated previously for an analogous dependence of P_c on $[Mg^{2+}]$ (*39*). That P_c tends to a nonzero value of 0.22 at increasing pH indicates that the $EM_{n+2}P_2$ species is catalytically active, i.e., k_4 and k_5 are greater than zero for this species. This means that protonation of $EM_{n+2}P_2$ to form $HEM_{n+2}P_2$ is modulatory rather than essential for catalysis. This and similar effects of proton removal from HEM_2 (modulation of metal ion binding) and $HEM_{n+2}PP^*$ (modulation of k_3) are likely to result from a change in protein structure and may be controlled by a single protein group, whose pK_a is affected by active site bound ligands.

An important conclusion stemming from comparison of the pK_a values in Scheme 3 is that substrate binding and isomerization of $HEM_{n+2}PP^*$ to $HEM_{n+2}PP$ facilitate removal of proton from the essential basic group by increasing its acidity. The most likely candidate for this group is a water molecule bridging the metal ions M1 and M2 and, presumably, acting as the nucleophile at the k_3 step (*2*, *13*, *14*). In this case, substrate binding and the isomerization of the resulting complex both serve to activate the nucleophile by converting it into a more reactive hydroxide.

Unlike other functions, the rate of PP_i release from its two complexes with Y-PPase ($k_{pp,off}$) increased dramatically with decreasing pH (Figure 3A). In terms of Scheme 1, $k_{pp,off}$ estimates the lower limit for k_2 (corresponding to $k_B \gg k_2$, k_A) and is given by eq 8, which can be reduced to $k_{pp,off} \approx k_B/(1 + k_A/k_2)$, as $k_2/k_B > 50$ (*10*). The ratio k_A/k_2 is close to unity at pH 7.2 (*10*), but a substantial effect on $k_{pp,off}$ might result if k_A/k_2 would change with pH. However, parameters k_A and k_2 refer to the same intermediate ($EM_{n+2}PP^*$ in Scheme 1) and their ratio is expected to be pH independent. If so, the pH dependence of $k_{pp,off}$ mirrors that of k_B. The correctness of this assumption is proven by the finding that the pH-profile of $k_{pp,off}$ is perfectly described by a pH-function containing only the K_a values for $EM_{n+2}PP$, to which k_B refers (Figure 3A). Thus, the reverse isomerization step (rate constant k_B), which is rate limiting in PP_i release, proceeds most rapidly from $H_2EM_{n+2}PP$, whereas PP_i hydrolysis (rate constant k_3) proceeds most rapidly from $HEM_{n+2}PP$ (Table 5). As a result, proton binding to $HEM_{n+2}PP$ stimulates PP_i release over its hydrolysis. A similar proton switch may operate in the mechanism of H^+-driven enzyme-catalyzed synthesis of PP_i (*40*) and ATP (*41*) in membrane systems.

$$k_{pp,off} = \frac{1}{1/k_B + 1/k_2 + k_A/k_Bk_2} \qquad (8)$$

Earlier kinetic analyses performed at a fixed pH 7.2 showed that catalysis of PP_i hydrolysis proceeds with either four or three metal ions bound (*8*, *11*). Here we demonstrate that the reaction involves as much as four catalytically competent enzyme−substrate complexes over wide ranges of Mg^{2+} and H^+ concentrations (Scheme 2B). HEM_3S is the most efficient among them, indicating that $MgPP_i$ is hydrolyzed more rapidly than Mg_2PP_i. Binding a fourth metal ion or removing a proton both decrease k_h, the effects being additive (Table 3). The three-Mg route is also faster in PP_i synthesis, whereas P_i/H_2O oxygen exchange and enzyme-bound-PP_i formation are most efficient with four Mg^{2+} ions bound (*8*). That $v_s/[E]_t$ monotonically increases with increasing $[Mg^{2+}]$ at fixed total P_i concentration (Table 4) is explained by the increase in the concentration of MgP_i complex, which is weakly bound substrate in the synthesis reaction.

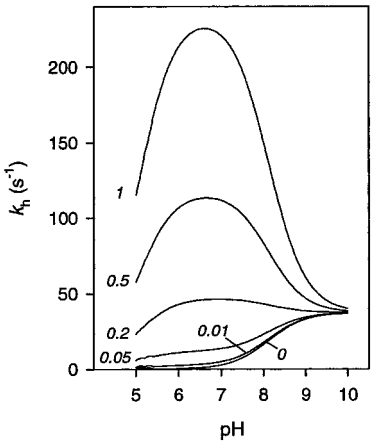

FIGURE 6: pH dependencies of k_h simulated with eq 4. Parameter values were taken from Table 3, except for $k_h^{(1)}$ and $k_h^{(2)}$, for which the values shown in Table 3 were further multiplied by the factors shown at the curves. Mg^{2+} concentration was fixed at 20 mM.

The multiplicity of active enzyme−substrate complexes provides an alternative explanation for the observation that conservative mutations of many active site residues in Y-PPase (*14*) and E-PPase (*13*) increase by several units the apparent pK_a of the essential basic group seen on k_h versus pH profiles obtained at 20 mM Mg^{2+}. It was suggested that this effect arises from an increase in a presumably low pK_a of the nucleophilic water because of distortion of the delicate network of interactions in the active site. An alternative suggestion is that the variants with significantly distorted active site structure require the whole complement of the four metal ion to restore catalytically competent structure, but are inactive with three metal ions bound (i.e., $k_h^{(1)}$ and $k_h^{(1)*}$ in Scheme 2B are equal to zero). As shown in Figure 6, canceling the three-metal route suffices to shift the pH dependence by about 2 pH units, decrease the maximum k_h value, and eliminate the decrease in k_h at high pH, as was observed for a number of Y-PPase variants (*14*). In accordance with this suggestion, several E-PPase variants with elevated basic group pK_a are active only with four metal ions bound (*12*, *16*). Of course, it is possible that both suggested mechanisms are operative in particular PPase variants.

To sum up, the pH dependence of Y-PPase catalysis suggests that the isomerization of the enzyme·PP_i intermediate activates the water nucleophile by decreasing its pK_a from > 7.0 to 5.8. Deprotonation of another group, with a pK_a of 8−9, modulates this and several other steps, presumably through a change in protein structure.

REFERENCES

1. Kolakowski, L. F., Schlösser, M., and Cooperman, B. S. (1988) *Nucleic Acids Res. 16*, 10441−10452.

2. Heikinheimo, P., Lehtonen, J., Baykov, A. A., Lahti, R., Cooperman, B. S., and Goldman, A. (1996) *Structure 4*, 1491−1508.
3. Teplyakov, A., Obmolova, G., Wilson, K. S., Ishii, K., Kaji, H., Samejima, T., and Kuranova, I. (1994) *Protein Sci. 3*, 1098−1107.
4. Leppänen, V.-M., Nummelin, H., Hansen, T., Lahti, R., Schäfer, G., and Goldman, A. (1999) *Protein Sci. 8*, 1218−1231.
5. Kunitz, M. (1952) *J. Gen. Physiol. 35*, 423−450.
6. Baykov, A. A., and Avaeva, S. M. (1973) *Eur. J. Biochem. 32*, 136−142.
7. Welsh, K. M., Jacobyansky, A, Springs, B., and Cooperman, B. S. (1983) *Biochemistry 22*, 2243−2248.
8. Baykov, A. A., and Shestakov, A. S. (1992) *Eur. J. Biochem. 206*, 463−470.
9. Harutyunyan, E. H., Kuranova, I. P., Vainshtein, B. K., Höhne, W. E., Lamzin, V. S., Dauter, Z., Teplyakov, A. V., and Wilson, K. S. (1996) *Eur. J. Biochem. 239*, 220−228.
10. Baykov, A. A., Fabrichniy, I. P., Pohjanjoki, P., Zyryanov, A. B., and Lahti, R. (2000) *Biochemistry 39*, 11939−11947.
11. Springs, B., Welsh, K. M., and Cooperman, B. S. (1981) *Biochemistry 20*, 6384−6391.
12. Fabrichniy, I. P., Kasho, V. N., Hyytiä, T., Salminen, T., Halonen, P., Dudarenkov, V. Yu., Heikinheimo, P., Chernyak, V. Ya., Goldman, A., Lahti, R., Cooperman, B. S., and Baykov, A. A. (1997) *Biochemistry 36*, 7746−7753.
13. Salminen, T., Käpylä, J., Heikinheimo, P., Kankare, J., Goldman, A., Heinonen, J., Baykov, A. A., Cooperman, B. S., and Lahti, R. (1995) *Biochemistry 34*, 782−791.
14. Pohjanjoki, P., Lahti, R., Goldman, A., and Cooperman, B. S. (1998) *Biochemistry 37*, 1754−1761.
15. Baykov, A. A., Artjukov, A A., and Avaeva, S. M. (1976) *Biochim. Biophys. Acta 429*, 982−992.
16. Käpylä, J., Hyytiä, T., Lahti, R., Goldman, A., Baykov, A. A., and Cooperman, B. S. (1995) *Biochemistry 34*, 792−800.
17. Baykov, A. A., Hyytiä, T., Volk, S. E., Kasho, V. N., Vener, A. V., Goldman, A., Lahti, R., and Cooperman, B. S. (1996) *Biochemistry 35*, 4655−4661.
18. Borshchik, I. B., Magretova, N. N., Chernyak, V. Ya., Sklyankina, V. A., and Avaeva, S. M. (1986) *Biokhimiya 51*, 1484−1489.
19. Efimova, I. S., Salminen, A., Pohjanjoki, P., Lapinniemi, J., Magretova, N. N., Cooperman, B. S., Goldman, A., Lahti, R., and Baykov, A. A. (1999) *J. Biol. Chem. 274*, 3294−3299.
20. Heikinheimo, P., Pohjanjoki, P., Helminen, A., Tasanen, M., Cooperman, B. S., Goldman, A., Baykov, A., and Lahti R. (1996) *Eur. J. Biochem. 239*, 138−143.
21. Bradford, M. M. (1976) *Anal. Biochem. 72*, 248−254.
22. Baykov, A. A., and Avaeva, S. M. (1981) *Anal. Biochem. 116*, 1−4.
23. Nyrén, P., and Lundin, A. (1985) *Anal. Biochem. 151*, 504−509.
24. Baykov, A. A., Bakuleva, N. P., and Rea, P. A. (1993) *Eur. J. Biochem. 217*, 755−762.
25. Smirnova, I. N., Shestakov, A. S., Dubnova, E. B., and Baykov, A. A. (1989) *Eur. J. Biochem. 182*, 451−456.
26. Smith, R. M., and Alberty, R. A. (1956) *J. Am. Chem. Soc. 78*, 2376−2380.
27. Childs, C. W. (1970) *Inorg. Chem. 9*, 2465−2469.
28. Duggleby, R. (1984) *Comput. Biol. Med. 14*, 447−455.
29. Baykov, A. A., Hyytiä, T., Turkina, M. V., Efimova, I. S., Kasho, V. N., Goldman, A, Cooperman, B. S., and Lahti, R. (1999) *Eur. J. Biochem. 260*, 308−317.
30. Hackney, D. D. (1980) *J. Biol. Chem. 255*, 5320−5328.
31. Swaminathan, K., Cooperman, B. S., Lahti, R., and Voet, D. (1997) Brookhaven Protein Data Bank, filename 1huk.
32. Ridlington, J. M., Yang, Y., and Butler, L. G. (1972) *Arch. Biochem. Biophys. 153*, 714−725.
33. Ridlington, J. M., and Butler, L. G. (1972) *J. Biol. Chem. 247*, 7303−7307.
34. Baykov, A. A., Tam-Villoslado, J. J., and Avaeva, S. M. (1979) *Biochim. Biophys. Acta 569*, 228−238.
35. Kankare, J., Salminen, T., Lahti, R., Cooperman, B., Baykov, A. A., and Goldman, A. (1996) *Biochemistry 35*, 4670−4677.
36. Harutyunyan, E. H., Oganessyan, V. Yu., Oganessyan, N. N., Avaeva, S. M., Nazarova, T. I., Vorobyeva, N. N., Kurilova, S. A., Huber, R., and Mather, T. (1997) *Biochemistry 36*, 7754−7760.
37. Avaeva, S. M., Rodina, E. V., Kurilova, S. A., Nazarova, T. I., Vorobjeva, N. N., Harutyunyan, E. H., and Oganessyan, V. Yu. (1995) *FEBS Lett. 377*, 44−46.
38. Calvo, C. (1967) *Acta Crystallogr. 23*, 289−295.
39. Kasho, V. N., and Baykov, A. A. (1989) *Biochem. Biophys. Res. Commun. 161*, 475−480.
40. Baltscheffsky, M., and Baltscheffsky, H. (1992) in *Molecular mechanisms in bioenergetics* (Ernster, L., Ed.) pp 331−348, Elsevier, Amsterdam.
41. Boyer, P. D. (1997) *Annu. Rev. Biochem. 66*, 717−749.

BI000895S